



Energy and Environmental Analysis of Solar Air Cooling with 2-Stages Adsorption Chiller in Jordan

Mohammed Issa Shahateet*, Ghani Albaali, Abdul Ghafoor Saidi

Princess Sumaya University for Technology, Jordan. *Email: msh@psut.edu.jo

Received: 05 June 2021

Accepted: 28 August 2021

DOI: <https://doi.org/10.32479/ijeep.11701>

ABSTRACT

The objectives of this study are to examine the use of the technology of Cooling Air by Solar Energy (CASE), which is used in air-conditioning applications to minimize the consumption of energy, as well as minimize CO₂ emissions. The study also aims at providing an overview of different CASE technologies and analyzing the environmental feasibility of selected CASE technologies in Jordan. The methodology used involves a field study of one of the CASE technologies, which has been designed and developed in Jordan, to determine its technical feasibility. The environmental feasibility study has been done on the device used in this work in four scenarios. The results of the analysis of both energy and environmental feasibility have shown that the use of the CASE technology reduces greenhouse gases compared with Vapor Compression Chillers (VCC) that use electricity.

Keywords: Solar Air-cooling, Vapor Compression Chillers, Greenhouse Gases, Energy Analysis

JEL Classifications: P18, Q40, Q43, Q51

1. INTRODUCTION

The future supply of energy in Jordan is of high concern, and it is completely dependent on imported oil and its products. Jordan's growing demand for air conditioning necessitates the use of Vapor Compression Chillers (VCC). These systems have a remarkable adverse effect on the environment in two ways: by increasing CO₂ emissions due to the increase in the consumption of energy and by causing ecological problems due to refrigerant use. While the refrigerants used in normal refrigeration cycles no longer have a potential for Ozone Depletion (OD), they do have a significant potential for Global Warming (GW) due to chiller leakage. Climate change-related temperature increases will raise the load on cooling in the future, consuming higher energy for air conditioning. All of the preceding points indicate that CASE has the potential to significantly reduce electricity consumption and greenhouse gas emissions. Jordan currently has only two AC building systems in operation, the Aqaba Residency Energy Proficiency (AREP) and the Dead Sea Hotel and Spa, with theoretical cooling capacities of 10 kW and 17.5 kW, respectively. This is because of the high

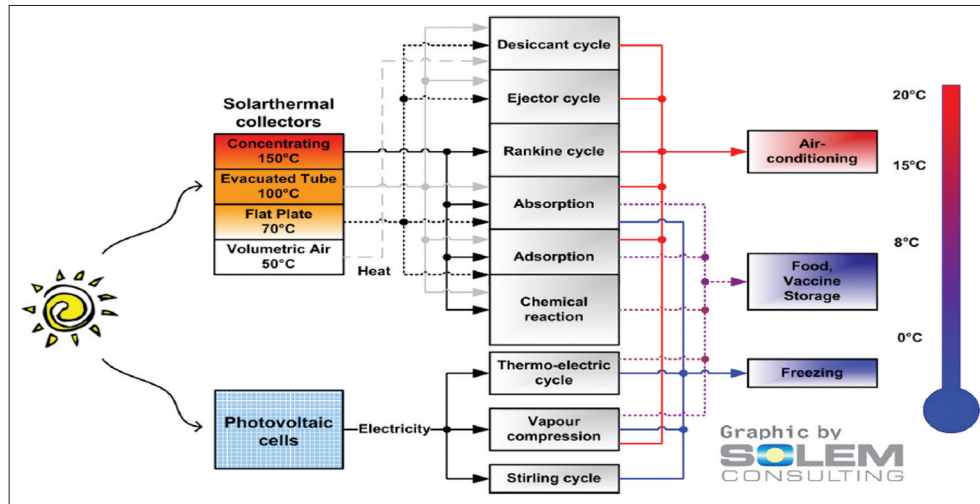
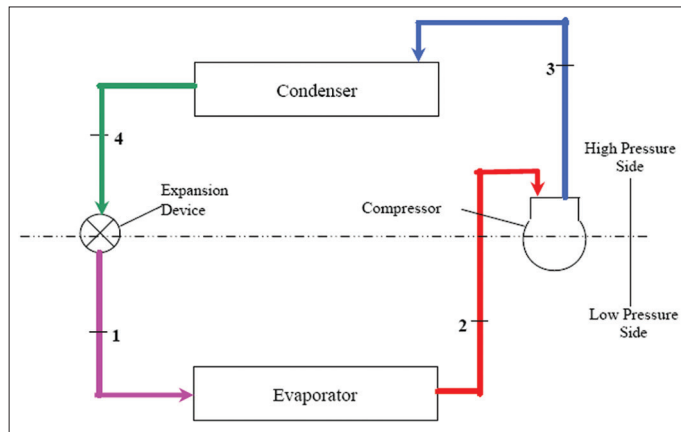
technical difficulties associated with such systems, which are designated for the conditions of European weather, which differ from those in Jordan, and, finally, the shortage of local experience with CASE technology.

1.1. CASE Technology

Solar air cooling systems can be divided into two broad groups based on how solar radiation is converted physically: electrical and thermal systems.

Figure 1 shows, only 3 distinct types of commercially solar cooling systems are available: adsorption and absorption chillers, as well as, desiccant systems. The most frequently used cooling cycle is vapor-compression cooling. Refrigeration is propelled forward by mechanical energy. Thermal energy is used as the driving force for refrigeration in small absorption and adsorption chillers. The refrigeration cycle depicted in Figure 2 is classified as follows:

1. The evaporator's refrigeration of the liquid with low pressure absorbs heat from the circumference, which is typically air, water, or another processing liquid

Figure 1: Transformation of the solar radiation in solar cooling

Figure 2: The refrigeration cycle


2. The superheating vapor gets in the compressor, which leads to an increase in its pressure. Temperatures will also rise because of the refrigerant absorbing a portion of the energy used in the compression process
3. The subcooled liquid of high-pressure flows by the expansion unit, which decreases the pressure simultaneously and regulates its flow to the evaporator.

The small applications of available chiller products are referring to the term “small,” which is for the chilling system of the capacity of lower than 20 kW. VCC efficiency is expressed as the Coefficient of Performance of VCC (CP_{VCC}), which can be introduced as the effect of refrigeration divided to be the input of electrical power, both measured in kW.

$$CP_{VCC} = Q_c / EP_{input} \quad (1)$$

where Q_c is the capacity of cooling, EP_{input} is the input of electrical power. The CP_{VCC} relies on the difference in pressure between condenser and evaporator and thus on the difference in temperature between them. The higher difference in temperature will reduce the CP_{VCC} . This is why the possible lower difference in temperature is advantageous because of the reduction in the consumption of energy.

$$CP_{VCC} = 3.6 - 0.06 (t_a - t_{ch,in}) \quad (2)$$

Where $t_{ch,in}$ is the temperature of chilled water of inlet, and t_a is the ambient temperature.

1.2. Solar Cooling

Different thermal solar collectors are used as a source of a thermal driven chiller, which considers as the fundamental idea of thermal CASE, (Figure. 3).

AC air cooling, CW chilled water, HD heat driving, HR heat rejection, SC solar cooling, TDC thermal driven chiller and CT cooling tower.

TDC depicts the thermodynamics cycle where heat is absorbed in one level of temperature, raised to a high level of temperature, and then rejected. The CP of CASE system or chiller-driven thermally is split into two types shown in the following equations:

$$CP_{E,CASE} = Q_c / P_{E,CASE} \quad (3)$$

$$CP_{T,CASE} = Q_c / Q_H \quad (4)$$

where

$CP_{E,CASE}$ is the electrical CASE CP

$P_{E,CASE}$ is the CASE system electric consumption

$CP_{T,CASE}$ is the thermal CASE CP

Q_c is the chiller cooling capacity

Q_H is the heat drive

1.3. Absorption Chillers

Absorption chillers are machines units that produce chilled water by using heat, such as hot water, steam, gas, etc., and they consist of an absorber, a pump and a generator. The absorber is used to absorb refrigeration vapor by the appropriate absorber and form a strong solution of refrigerant. The pump is used to increase the pressure to that for condenser by pumping the strong solution of the absorber, as well as, the generator which distilled the vapor from the strong solution. The principle of operating the absorption chiller is similar to those for normal VCC. These 3 units (absorber, pump, and generator) are instead of VCC compressor (Srikhirin et al., 2001).

Absorption chillers are divided into two categories, which are:

1. Single-effect cooling systems that use thermal energy to power a single refrigeration cycle. It is commonly convenient for applications at lower temperatures, probably about 75–132°C
2. Systems of double-effect cooling that use two refrigeration cycles. The first and second cycles are driven respectively by the higher temperature thermal energy and the low-temperature energy rejected by the condenser of the former cycle. These systems need steam at about 190°C and a pressure of 900 kPa (Grossman, 2002). The comparison of vapor absorption technology is shown in Table 1.

Another classification for these systems could be made according to the refrigerant-absorbent pairs. Two mostly used refrigerant-absorbent pairs are lithium bromide (LiBr) as a solvent and water and ammonia and water as a refrigerant.

ADCs are split into two denominations, single and two-stage chillers. Figure 4 shows the condenser, evaporator and two sorbent compartments of single-stage ADC (ECO-MAX, 2011).

Table 2 presents the specifications of ADCs available in markets.

The scheme of the function of 2-Stages Adsorption Chiller (ADC-2) is shown in Figure 5 below:

The cooling unit of ADC-2 is composed of a condenser with in/out end, evaporator with in/out end and chain of the generator of sorption adsorption with in/out end to connect to the evaporator and condenser. This chain of generations consists of 2 pairs of generations as follows (Al-Maaitah and Al-maaitah, 2013):

1. The first generator with in/out ends connected to the condenser input end through the first Non-return Valve (NRV)
2. The second generator with in/out ends connected to the condenser input end through the second NRV.

The above configuration is to restrain the flow from the condenser to the first generator. The second generator is equipped with the following features:

- Evaporator’s input end is connected to the output end through a second NRV. Such arrangement prevents the second generator from feeding the evaporator

Table 1: Vapor absorption technologies

System	Operating temp. (°C)		WF	CCAP (ton)	CP
	Heat source	Cooling			
SEC	80–110	5–10	LiBr/water	10–100	0.5–0.7
DEC	120–150	<0	Water/NH3	3–25	0.5
	120–150	5–10	LiBr/water	up to 1000	0.8–1.2

SEC and DEC is single and double effect cycle respectively, WF working fluid, CCAP cooling capacity and CP is the coefficient of proficiency, (Srikhirin et al., 2001)

Table 2: Available adsorption chillers in the market

Operating temp. (°C)	WF	CCAP (ton)	CP
65–95	Water/silica gel	7.5–350	0.6

- The output end of the first generator is connected to the input end through a third NRV. Such arrangement prevents the second generator from feeding the evaporator, and this prevents the flow from the input of the first generation to the output of the second.

Every pair of generations can operate independently to drive the fluid through the evaporator and condenser and provides cooling. Table 3 shows the absorption versus adsorption chillers

Figure 3: Basic principle of thermal driven systems

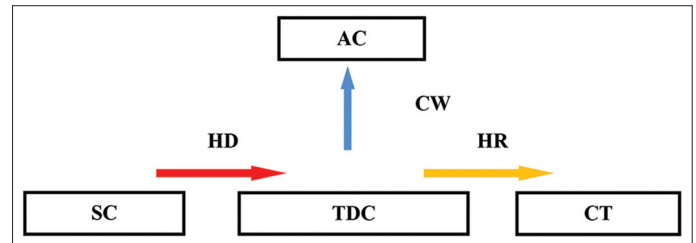


Figure 4: Condenser, evaporator and two sorbent compartments of the single-stage adsorption chiller

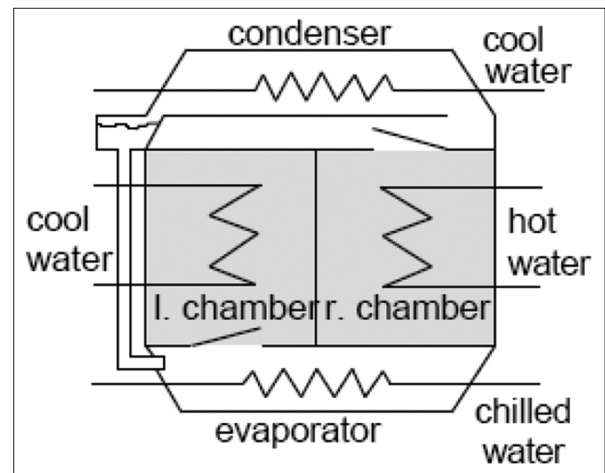
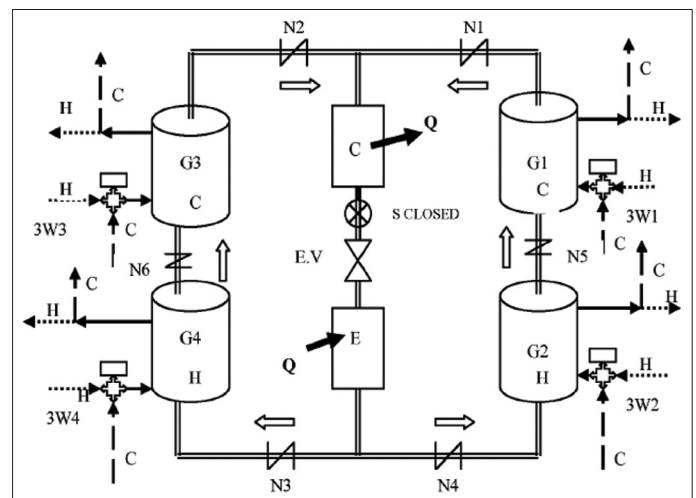


Figure 5: 2-Stages Adsorption Chiller ADC-2, showing evaporator, condenser and the four sorbents



EV is Expansion Valve, G's are Generators, N's are Non-Return Valves, and 3W's are the 3-Way Valves allowing water (hot or cold) to enter generators

Table 3: Absorption versus adsorption chillers

Attribute	Absorption chiller	Adsorption chiller
Continuous operation	Dilution of lithium bromide solution daily shutdown maintenance	Possibility of continuous operation for more than 8000 h/year
Time for startup and shutdown	Dilution cycle required. Startup and shutdown times vary with the manufacturer	No requirement for a specific procedure. Reach to full capacity in a maximum of 8 min without any negative impacts from losing power
Chemistry	Distilled water and lithium-bromide	Municipal water and silica gel
Requirements of hot water	The variation should be strongly controlled between the temperature 180°F and 212°F or higher than that. If hot water is lower than 175°F then backup heat is required to prevent crystallization	Continuously variable, Between 122°F and 205°F or higher; simply automatic shutdown at 122°F
Requirements of cooling for water	The temperature should be between 65°F and 85°F and by the use of a control valve	Low temperatures between 85°F to 50°F enlarge the system's capacity
Chilled water output	48°F or warmer	Between 40°F and 55°F is normal
Freq. of desiccant replacement	Every 4–5 years	Not necessary
End of life requirements	Needs a procedure for the disposal of hazardous materials	No special disposal requirements

Source: ECO-MAX, 2011

The main advantageous of ADC-2 are:

- Operation at high temperature (50°C and over)
- Comfortable drive to the temperature from 70°C to 95°C
- A simple technique for heat rejection and no consumption of water.

2. REVIEW OF LITERATURE

The new inventions in solar energy use in civil societies were a major turning point in preserving the environment and reducing CO₂ emissions. These inventions were the major topics in scientific research studies that dealt with energy and environmental analysis of solar air cooling. However, several themes are seen in these studies. Fu et al. (2021), for example, investigated an advanced adiabatic compressed air energy storage system with a variable pressure ratio based on the organic Rankine cycle to improve the cycle efficiency of compressed air energy storage. The system's thermodynamic model is established and used to calculate the system's thermodynamic characteristics. The results indicate that when compared to advanced adiabatic compressed air energy storage, the system with a variable pressure ratio reduces compression process power consumption by 12.45% and increases expander output power by 37.29%, increasing the cycle efficiency of the system from 40.16% to 63.00%.

On the other hand, Ma et al. (2019) took a cost-benefit analysis approach to determine the optimal integration of the recompression CO₂ Brayton cycle with main compression inter-cooling. Sensitivity analysis demonstrates the effect of solar component cost and design on the optimal integration of the CO₂ cycle and indicates that under certain solar component cost and design conditions, the optimal cycle layout may degrade from the recompression cycle to a simple recuperating cycle. Zhang et al. (2019) also developed a model based on the characteristics of a real wind farm with a capacity of 49.5 MW in China. According to Medel results, it was possible to increase the compressor and expander operational ranges of the proposed system by 70.85% and 27.27%, respectively. Additionally, the results indicate that after integration with the specified system, wind power (average: 21.05 MW) with fluctuations up to 49.5 MW can be stabilized to a steady electric power of 18.64 MW, increasing the wind power utilization coefficient from 26.29% to 71.02%. Ratlamwala and Abid (2018) conducted a performance comparison of absorption refrigeration systems with multiple effects. Solar heat is used to power the absorption cooling cycles, which maximizes the utilization of high-temperature heat sources for absorption systems. The multi-effect absorption refrigeration cycles are modelled and designed for identical refrigeration capacity and operating conditions. The engineering equation solver is used to determine the coefficient of performance (COP) and the energy efficiency of absorption cooling cycles. Simulations of performance under a variety of operating conditions were conducted, including the effect of heat transfer fluids (nanofluids) used in solar parabolic trough collectors. The triple effect absorption refrigeration cycle has a coefficient of performance of 1.752. The double effect absorption refrigeration cycle is perceived to have a higher coefficient of performance (51.9%) than the single effect absorption refrigeration cycle, which has a coefficient of performance of 0.852.

Another study investigated the use of an advanced metal-organic framework adsorbent material, in a one-bed adsorption system for water desalination and cooling applications using both experimental and numerical methods. The effect of operating parameters on cycle water production and cooling was investigated. They created a mathematical simulation model to forecast cycle outputs under a variety of different operating conditions. Cycle outputs increased as evaporator temperature increased and condenser temperature decreased. Additionally, it was demonstrated that open-loop adsorption desalination cycles can operate with a condenser pressure less than the evaporator pressure (Youssef et al., 2017). In another strand, Kojok et al. (2016) investigated one of the hybrid cooling systems that are an energy-efficient method of cooling buildings. The study concluded that a properly chosen hybrid cooling system can significantly reduce energy consumption and improve performance by a coefficient of performance improvement that varies according to climate and system design. They conduct an in-depth examination of existing hybrid cooling systems and their associated individual cooling machines. To begin, a brief overview of the state of the art for the most common individual cooling systems used in hybrid cooling for building use is provided. Then, based on the combination of cooling

processes or machines, hybrid cooling systems are classified into five broad categories: vapor compression-based cooling, absorption-based cooling, adsorption-based cooling, desiccant-evaporative cooling, and multi-evaporator cooling. The studied configurations and the advantages of each hybridization method are presented in each category. Each hybrid system is found to combine the advantages of the various cooling processes used. However, a hybrid system may have negative consequences if it is not appropriate for the climatic zone in which it will be used. Giwa et al. (2016) demonstrate the enormous economic and environmental benefits of HDH technology by examining recent advances in humidification dehumidification (HDH) desalination processes. This paper discusses the primary HDH components, the latest research on HDH systems powered by renewable energy, and recent innovations in HDH design for sustainable water production. It is worth noting that the key characteristics and sustainability aspects of HDH desalination technology are still being developed, and additional improvements are required to optimize process performance parameters such as the quantity of water produced, specific renewable energy required, and specific cost of water produced. However, HDH technology has been demonstrated to be an affordable and environmentally friendly desalination system for small-scale applications.

Grossman (2002) discusses solar-powered air-conditioning trends. The study confirms that closed-cycle heat-powered cooling devices are primarily absorption chillers, a well-established technology that utilizes the working fluid pair LiBr–water. These systems, however, necessitate the use of high-temperature solar collectors. The fundamentals of multiple-stage absorption systems are discussed. Economic analysis reveals that the solar component of the system accounts for the lion's share of the total system cost. Additionally, it demonstrates that the high-temperature alternative is still more expensive than the low-temperature alternative.

In sum, evaluating these strands in the literature indicates that their application was limited to developed countries or they focused on a theoretical setting. This study, while emphasizing the theoretical methodology, concentrates on the application of using solar air cooling with a 2-stages adsorption chiller in a developing country: Jordan, and hence contributes to knowledge in this area of research.

3. METHODOLOGY

Evaluation of installed prototype at Aqaba weather condition has been done to determine and analyze the technical feasibility for the operating of ADC-2 cooling systems and their performance, taking into consideration that the average maximum temperature is more than 40 degrees Celsius in summer. Millennium Energy Industries (MEI) invented, developed, and manufactured this two-stage adsorption chiller prototype, which was successfully operated at their R and D lab in Amman under the conditions of extremely high temperature and high cooling temperature of the water. The primary reason for using CASE technology is to decrease the emissions of greenhouse gasses. As a result, the environmental analysis is used in this study to determine if the use of ADC-2 systems is feasible environmentally.

4. EXPERIMENTAL SETTING AND THEORY

To determine the technical function for the cooling system of ADC-2 and to analyze its effectiveness, the prototype setup in the Aqaba region (AR) was evaluated based on the weather conditions in Aqaba, where the average maximum temperature in summer reaches 40°C. Millennium Energy Industries (MEI) in Amman invented, developed, and manufactured this two-stage adsorption chiller prototype, which was successfully operated at its Research and Development laboratory under extreme weather conditions of hot weather and high cooling water temperature. To evaluate the ADC-2 installed at AR, extensive testing was conducted over 2 months (daily 4-6 h.) to determine the system's performance under varying temperature conditions, as well as, to determine system alteration required to maintain continuous operation. The conditions of chilled, hot and medium water inlet temp. ($T_{ch,in}$, $T_{h,in}$, $T_{m,in}$) into the chiller, were used to analyze the device's performance.

4.1. Equipment Used in the Study

The MEI ADC-2 pilot diagram installed in the Aqaba region is shown in Figure 6, which represents the major parts of the pilot project. This figure shows that the system consists of ADC-2, heat and heat rejection loops, cooling loop, all appliances including the monitoring unit.

4.1.1. ADC-2 unit

Figure 7 shows the MEI ADC-2 installed at Aqaba Region (AR). Based on the database, the chiller cooling capacity is 10 kW and the thermal CP is 0.33 at $T_{h,in}$, $T_{m,in}$, and $T_{ch,in}$ of water inlet, which was at temperatures of 90°C, 35°C, 18°C respectively.

4.1.2. Heating unit

15 Evacuated tube parabolic solar water concentrators (Limo Paradigm) were installed at Aqaba region (Figure 8). These Solar Water Collectors (SWC) were lying at a tilt angle (15°) to achieve the highest solar radiation, specifically during the summer season. These solar water collectors were supplied with a hot water system at 70°C-90°C for 4-6 h/day in summer. This is in addition to 24 h daily of providing hot water demand. These SWCs were connected to a storage tank of 500l to avoid inconsistency as well as to provide hot water at night.

Figure 6: Diagram of the 2-stages adsorption chiller at AREP

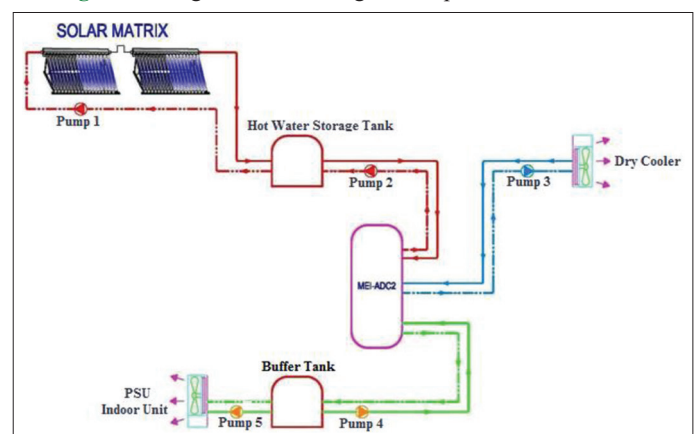


Figure 7: MEI ADC-2 installed at AR

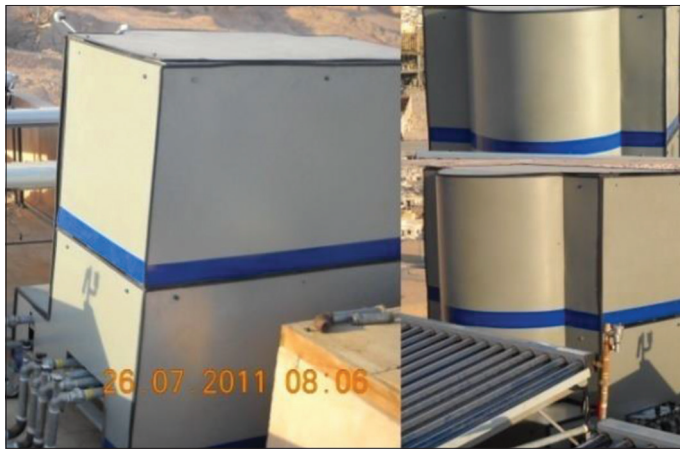


Figure 8: Solar water heaters installed at AR



Figure 9: Dry Cooler installed at AR



- Electromagnetic flow meters ($\pm 4\%$ accuracy) were connected to the screen to show the reading of the flow. The readings of temperature and flow were displayed and saved on a laptop computer (Figure 10c).

4.2. Energy Analysis: Theory

Energy balance analysis is presented in this work, which is needed to have the data required in the performance analysis. The terms and equations that will explain the energy balance needed for this case study are shown below. Figure 11 presents the MEI ADC-2 Energy flow for the integrated and chilling systems at the Aqaba region.

From the above diagram, the equation of energy balance for the chiller is as follows:

$$Q_{Rej} = Q_H + Q_C \quad (5)$$

where Q_{Rej} is the heat reject, Q_H is the heat drive, and Q_C is the chiller cooling capacity.

Chiller's cooling capacity can be measured using below equation (6):

$$Q_C = m_{ch} \times C_{p_{ch}} \times \Delta T_{ch} \quad (6)$$

Where $C_{p_{ch}}$ is the chilled water specific heat measured at a fixed pressure, m_{ch} is the rate of mass flow of chilled water, and ΔT_{ch} is the difference in temperature between the chiller inlet/outlet. The heat drive capacity can be measured using below equation (7):

$$Q_H = m_h \times C_{p_h} \times \Delta T_h \quad (7)$$

Where

m_h is the rate of mass flow of hot water
 C_{p_h} is the hot water specific heat measured at a fixed pressure
 ΔT_h is the difference in temperature between chiller inlet/outlet.

Several possibilities of heat sources, like solar energy, waste heat, and geothermal are available. In addition, there are several solar collectors available; most of those are usable in solar air cooling. The suitable type of these collectors relies on the

4.1.3. Cooling unit

The inlet/outlet water of the chiller is linked with a 150 L insulated tank to reduce the turmoil that might happen through the process and the bad control of temperature. The mentioned buffer tank manufactured locally is installed to minimize losses, and connected with the system of fan coil for the air conditioning.

4.1.4. Heat rejection unit

A dry cooler with a 40 kW capacity was installed at the Aqaba region (Figure 9). It is manufactured by a British Heat Exchangers Manufacturer (GEA Group). The dry cooler rejects the heat from the system released temperature to the surrounding temperature by the runtime to assure the continuity of the system's running.

4.1.5. Appliances and monitoring units

The appliances and monitoring system consist of:

- 3 water flow meters were employed for measuring the rate of the flow of hot, chilled, and medium water temperature loops (Figure 10a)
- 9 temperature sensors were employed for measuring the hot, chilled, and medium water temperature loops. The model of these sensors is TEP11 by Tecsis. The range of measurements for this type of sensor is from 0°C to 100°C with an accuracy of $<0.5\%$ of the range (Figure 10b).

Figure 10: (a) Water flow meter (b) Temperature sensor (c) Monitoring screen

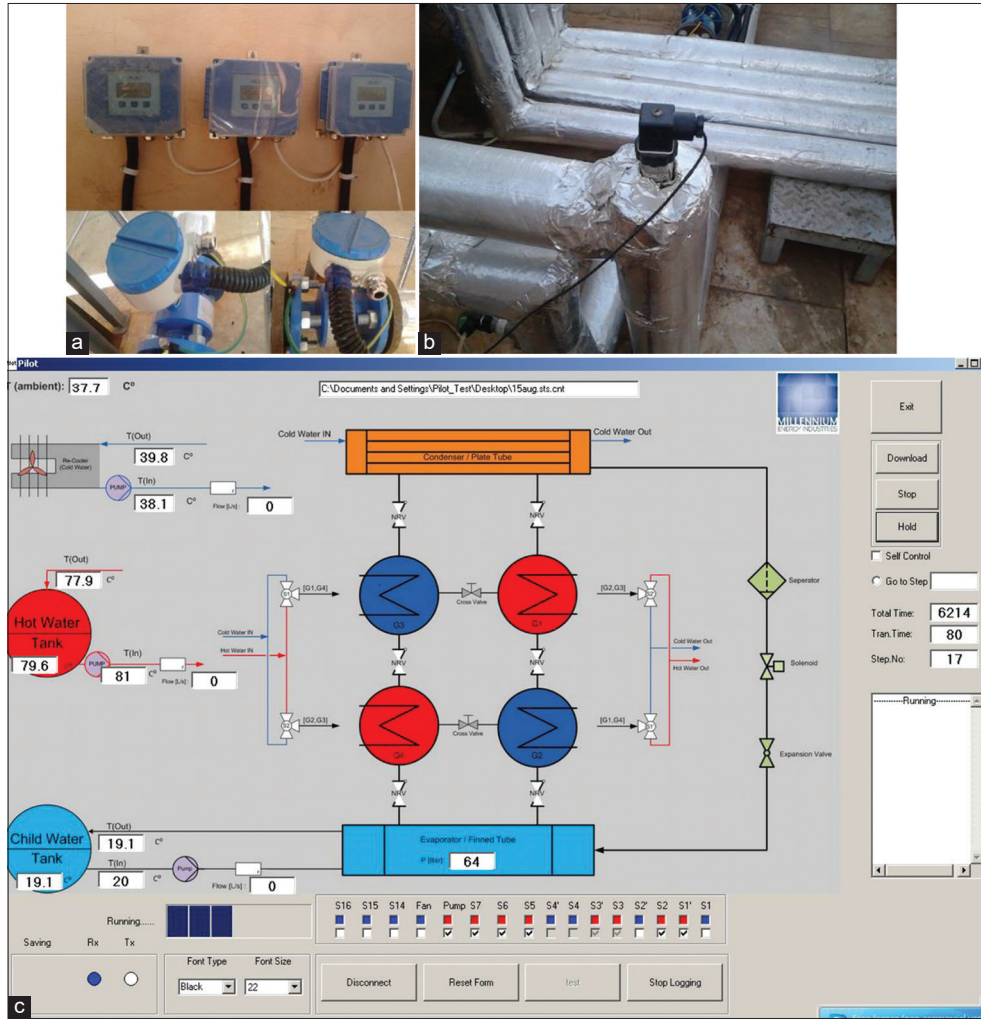
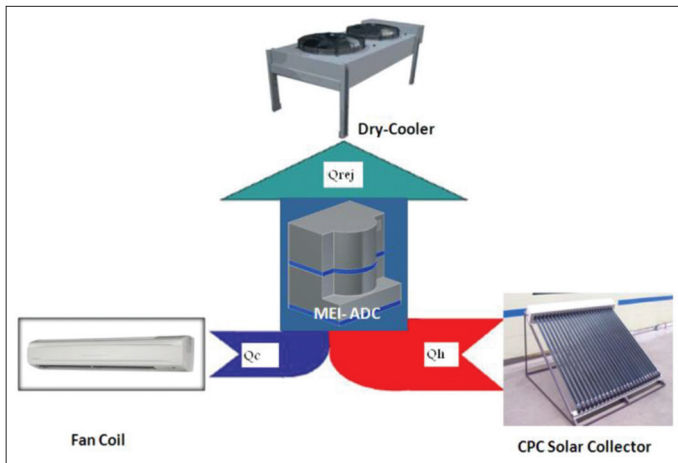


Figure 11: MEI ADC-2 Energy flow at Aqaba region



ected technology of cooling and surrounding temperature. Evacuated Tube Solar Collectors (ESC) with compound parabolic concentrators were used in this study. Equation 8 below is used to measure the area of the solar collector.

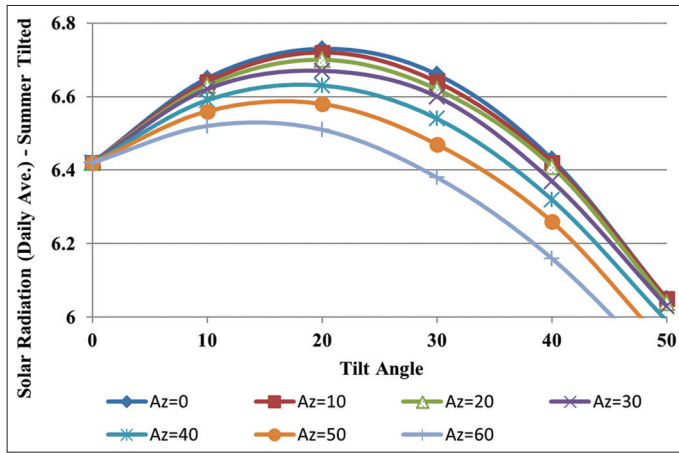
$$A = E / (SR \times \eta) \quad (8)$$

where A is the area, E is the energy, SR is the solar radiation, and η is the collector's efficiency. Solar radiation is generally depending on azimuth and tilt angles. This is why the SWC was oriented geographically and inclined (tilted) to receive the utmost amount of solar energy radiation on a daily and seasonal basis. The best tilt angle in the summer for the Aqaba region was taken from the RETSCREEN software, and it was 20° and 0° for tilt and azimuth angle, at tilted daily solar radiation in summer (February to November) of 6.73 kW-day/m^2 , and 4.18 kW-day/m^2 in winter (December and January). Figure 12 shows the average daily solar radiation tilt at summer versus azimuth and tilt angle at the Aqaba region.

The capacity of heat reject can be measured using below equation (9):

$$Q_{Rej} = m_m \times C_{p_m} \times \Delta T_m \quad (9)$$

where Q_{Rej} is the heat reject, m_m is the rate of mass flow of water medium temperature, C_{p_m} is the medium water temperature specific heat measured at a fixed pressure, and ΔT_m is the difference in temperature between the chiller inlet/outlet of medium water temperature.

Figure 12: Average of daily solar radiation tilt at summer versus azimuth and tilt angle AR


4.3. Analysis of Experimental Results

The chiller's thermal CP and cooling capacity at the conditions mentioned earlier is shown in Figure 13. The figure shows that the device is stable which means that it can adequately work with dry cooling at high temperature using low drive temperature, which can be easily accomplished, by the use of an evacuated tube collector. The results were in good agreement with those obtained in the lab at the same mentioned conditions.

For this case study, the acquired average cooling capacity is found of 4.8 kW comparing with 5.5 kW measured experimentally in the lab, which means that difference between the site measurements and the lab is around 12%. The reason for this difference in measurement is that the installed unit was in an area exposed to solar radiation and not shaded, which in turn resulting in a loss in the capacity of cooling due to it is positioned under solar radiation. The figure also shows that the average value of CP for the unit is 0.25, which is regarded too small compared with other technologies, that is due to the use of 2 units that can be operated at a higher ambient temperature.

The following equation represents the electrical energy consumption for the case study:

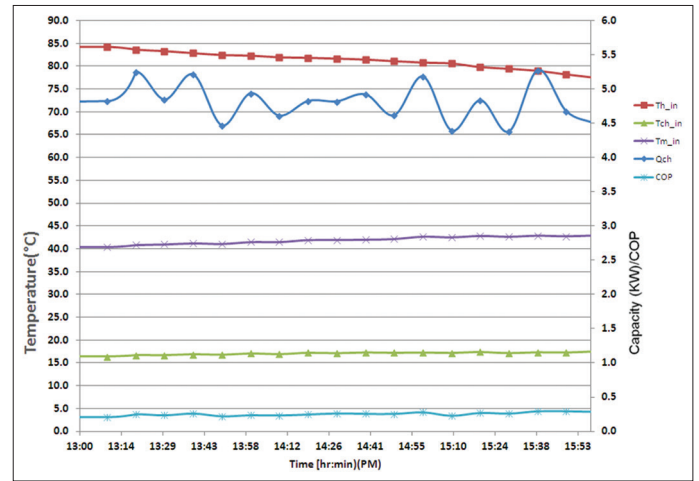
$$P_{E,CASE} = P_{rej} + P_{ch} + P_{chr} + P_h \quad (10)$$

where $P_{E,CASE}$ is the CASE system electric consumption, P_{rej} is the heat reject electric consumption, P_h is the heat drive electric consumption, P_{ch} is the chilled water electric consumption, and P_{chr} is the chiller electric consumption. The VCC consumption of electrical energy can be measured using below equation (11):

$$P_{E,VCC} = \frac{Q_c}{CP_{VCC}} \quad (11)$$

where

$P_{E,VCC}$ is the VCC system electric consumption
 Q_c is chiller cooling capacity
 CP_{VCC} is the coefficient of performance of VCC

Figure 13: Tested operating data of the MEI ADC-2 at AR


The save in the consumption of electric energy can be measured using the below equation (12):

$$\Delta PE = P_{E,VCC} - P_{E,CASE} \quad (12)$$

The consumption of real electric energy can be measured from the below equations (13 and 14).

$$P_{R,E,VCC} = \frac{P_{E,VCC}}{\zeta_g} \quad (13)$$

$$P_{R,E,CASE} = \frac{P_{E,CASE}}{\zeta_g} \quad (14)$$

where η_g is the efficiency of the electrical grid with T and D, $P_{R,E,VCC}$ is the real VCC system electric consumption, and $P_{R,E,CASE}$ is the real CASE system electric consumption. The fossil fuel save can also be measured if the heat reject from CASE is used to involve a load of heating, such as hot water for homes and industries, or other purposes, and when using the SWC for heating uses in winter. The saving in the consumption of diesel can also be measured if the diesel boiler is used to cover a load of heating, based on equation (15):

$$V_D = \frac{Q_{rej} \times \eta_{rej}}{H_{VD} \times \eta_{Boiler} \times \rho_D} \quad (15)$$

Where Q_{rej} is the heat reject, η_{rej} is the electric efficiency of the heat reject, V_D is the consumption of diesel, H_{VD} is the value of diesel heating, η_{Boiler} is the efficiency of the boiler, and ρ_D is the density of diesel, which is equal to 0.950 kg/L. According to the case study in this work, collectors should be inspected and cleaned every month, as dirt buildup on these collectors reduces their efficiency. As previously stated, one of the primary reasons for utilizing a CASE is to mitigate global warming caused by the emissions of greenhouse gasses accompanied by conventional system operation. The Potential of Global-Warming (PGW) is a relative measurement of the amount

of trapped heat in the atmosphere by greenhouse gas. The amount of trapped heat through a specific mass of a gas is compared to the quantity of trapped heat through comparable CO₂ mass. The below equation (16) is used to calculate the annual saving of CO₂:

$$CO_{2, \text{red}} = \left(\frac{\dot{A}PE_A}{CO_{2, \text{conv, elec}}} + \frac{Q_{\text{Rej}} \times Q_{\text{SWH}}}{CO_{2, \text{conv, D}}} \right) + H \quad \text{where}$$

CO_{2, red} is the carbon dioxide reduction measured in ton produced from the use of CASE technology, CO_{2, conv, elec} is the factor of the conversion of conventional electricity, and CO_{2, conv, D} is the factor of the conversion of fossil heat.

5. RESULTS AND ANALYSIS

In this section, different scenarios were assumed to check the environmental feasibility of ADC-2 based on the weather in Jordan. This has been done using RETSCREEN software package. The choice of the design and components for different scenarios were based on the following:

- A load of daily cooling is larger than the capacity of MEI ADC-2
- The rest of the load will be covered by VCC
- The cooling season in this study was assumed based on 10 months (February-November), while January and December are assumed for heating
- The calculations of temperature were assumed based on 32°C of surrounding temperature, and 18°C for the temperature of chilled water with laboratory test specifications of ADC-2 (Table 4).

5.1. First Scenario

The first scenario is assumed as follows:

- ADC-2
- Heat drive system
- Heat reject system
- Monitoring units.

The evacuated tube SWC model “CPC18” is used in this study. Based on the recommendations of the manufacturing company MEI, this collector is oriented with the best-tilted angle for the Aqaba region, as it is mentioned earlier. Table 5 shows the solar water collector SWC data.

The heat reject capacity of ADC-2 used is 40 kW, so a dry cooler of the same capacity is selected to keep the temperature medium water constant. A dry cooler model DXC 132H-EC215 manufactured by British heat exchangers manufacturer GEA is used in this work because of its high energy proficiency through the use of Electronic Commutated (ECOM) fans. The ECOM fan motors used are the same as a “shunt” motor that is brushless direct current motors (World Bank, 2014). Thus, with lesser loss, the Electronic Commutated motor is more proficient than the alternating current motor. Three pumps are needed for this system, which are the pumps for hot, medium, and chilled water, and it is postulated similar to that for VCC. Thus, the CW pump can be ignored from the calculation of this study. Table 7 below shows the required pumps technical specifications:

Table 4: MEI-ADC-2 technical data

Adsorption Chiller-2P High Ambient Temp. Operation System	
Factors	Values
Capacity of cooling	10 kW
Coefficient performance CP	0.34
Chilled water circuit	
Temp. Range (out)	15°C
Inlet temperature, T _{in}	18°C
Outlet temperature, T _{out}	15°C
Vol. flow	3 M ³ /h
Press. loss	250 mbar
Rejected heat circuit	
Temp. range (in)	20-50°C
Temp. (in/out)	35°C
Vol. flow	8.1 M ³ /h
Press. loss	500 mbar
Heat supply circuit	
Temp. range (in)	65-95°C
Inlet temperature, T _{in}	90°C
Vol. flow	4.5 M ³ /h
Press. loss	400 mbar
Electricity supply	
Voltage	230 Volt
Frequency	50 Hertz
Power	20 Watt
Dimensions	
Length × Width × Height	1000 mm × 1300 mm × 1600 mm
Weight	750 kg

Table 5: Solar water collector data

Compound parabolic concentrator-18	
Factors	Values
Aperture area	3 m ²
Optical efficiency η ₀	0.641
Collector heat-loss coefficient (W/m ² K), a ₁	0.886 Wm ⁻² K
Collector heat-loss coefficients (W/m ² K), a ₂	0.001 Wm ⁻² K
Operation conditions	
Inlet temp. (hot water), T _{in}	91°C
Outlet temp. (hot water), T _{out}	85°C
Mean temperature (hot water), T _{mean}	88°C
Ambient temperature, T _{ambient}	31°C
Tilt angle*	20°C
Cooling conditions	
Cooling	10kW
Coefficient performance CP	32%
Required thermal energy	30 kW
Operation time	8 h/day
Required thermal energy	243 kWh/day
Ave. peak of summer	6.72 kWh m ⁻² /day
Collector efficiency, η	0.58
Ave. peak of summer	11.55 kWh/Collector
No. of collectors	21

*Minimum acceptable to maximize summer season. The capacity of thermal energy resulted from these SWC in winter is 23 kW as shown in Table 6.

In this study, a “Wilco Stratus” model is used because it is highly efficient in power saving compared with other pumps. The software of the used pumps is to the choice of proper pump needed for this work. To regulate and check the effectiveness of the system, a monitor with flow meters for HW, MW, and CW are required to be utilized with temperature sensors for the inlet and outlet of all circuits. Tables 8 show the first scenario of electricity consumption.

5.2. Second Scenario

The difference between this scenario and the first one is in the method of heat rejection. The heat rejected in the first scenario is to the surrounding by the dry cooler, while the heat in the second scenario is not rejected to the surrounding but is used for heating the water and use for other purposes such as for domestic water uses, industries, swimming pools, and other applications depending on the heating water. This is due to the use of a heat exchanger. The consumption of electricity for the second scenario is similar to that in Table 8, except for the process of heat reject that is done by the use of an MW pump model “Stratos 40/1-12

Table 6: Thermal capacity of solar water collector at winter

Compound parabolic concentrator-18	
Aperture area	3 m ²
Optical efficiency η_0	0.643
Collector heat-loss coefficient (W/m ² K), a_1	0.886 Wm ⁻² K
Collector heat-loss coefficients (W/m ² K), a_2	0.001 Wm ⁻² K
Operation conditions	
Inlet temp. (hot water), T_{in}	86°C
Outlet temp. (hot water), T_{out}	71°C
Mean temperature (hot water), T_{mean}	78.5°C
Ambient temperature, $T_{ambient}$	21°C
Tilt angle	20°C
Heating conditions	
No. of collectors	21
Operation time	6 hrs./day
Ave. peak of summer	4.18 kWh m ⁻² / day
Collector efficiency η	0.54
Ave. peak of summer (of ea. Collector)	6.67 kWh
The capacity of thermal energy	23 kW

Table 7: Required pumps technical specifications

Specifications	HW Pump	MW Pump
Working temp.	90°C	45°C
Flow	4.5 m ³ /h	8.1 m ³ /h
Pressure drop in the chiller*	400 mbar	500 mbar
Pressure drop in the water pipes (assumption)	100 mbar	100 mbar
Pressure drop in the dry cooler/plate heat exchanger	130 mbar
Total pressure drop	500 mbar	730 mbar

HW and MW is the hot and medium water temperature

Table 8: First Scenario’s electricity consumption

Component	Elec. consumption (Watt)
Chiller	
MEI ADC-2	20.2
Heat driven	
Water pump (STC) Stratos Model 25/1 10 CANPN10	115
Water pump for hot water Stratos Model 25/1-10 CANPN 10	115
Heat reject	
Dry cooler model GEADDEC 233 - L6 EC030	150
Water pump (Medium) Stratos model 40/1 12 CANPN6/10	295
Total elec. consumption	695
$CP_{E,CASE}$	14.2
η_{SWH}	9912%

CAN PN6/10 with consumption of electricity equal to 296 Watt. This leads to the total consumption of electricity of 548 Watt rather than 695 Watt for the first scenario.

5.3. Third Scenario

The difference between this scenario and the first one is the source of heat drive. The heat drive in the first scenario arrives from SWC that was installed to drive the chiller, whereas the heat waste is used to operate the chiller in this scenario. The heat waste is usually produced by the production of steam, heating process, desalination of water, and industrial applications. In this investigation, the heat waste is presumed to arrive as hot water at a temperature value of 95°C. A 30 Kw energy heat exchanger will assist to use the heat waste to operate the chiller. A “SWEP B10T x 54” plate heat exchanger is chosen in this scenario. The consumption of electricity for the third scenario is similar to that in Table 8 above, except for the process of heat drive that is done by the use of the “B10Tx54” heat exchanger rather than SWC of 116 Watt of electric consumption that used in driving the chiller. This leads to a total consumption of electricity equal to 582 Watt comparing with 698 for the first scenario and with $CP_{E,CASE}$ of 17.2 Watt and η_{SWH} of 6873%.

5.4. Fourth Scenario

The difference between this scenario and the first one is the process of reject and drive the heat source. The rejection of heat is used to heat the water and use it for other purposes such as for domestic water uses, industries, swimming pools, and other applications, while in the source of heat drive, the waste of heat is used to drive the chiller. Table 9 shows the fourth scenario of electricity consumption.

The used software was conducted in the analysis of environment for different scenarios based on the following assumptions:

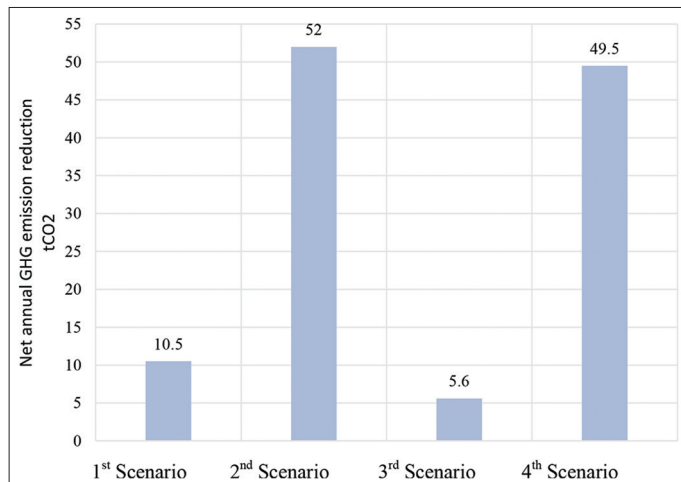
1. For the base case, VCC is the cooling system, with a CP of 2.78 as determined by Eq. 2
2. The base case heating system is a 60 per cent efficient diesel boiler.

The effect of GHG credits (carbon credits) is expected to be very strong when electricity prices are low, creating an extremely encouraging incentive for investment in CASE technology. It has been found that one of the main stimulations of CASE technology is its lower impact on the environment compared with VCC

Table 9: Fourth scenario’s electricity consumption

Component	Electricity consumption (Watt)
Chiller	
MEI ADC-2	20.2
Heat driven	
Water pump for hot water Stratos Model 25/1-10 CANPN 10 115	115
Heat reject	
Water pump (Medium) Stratos Model 40/1 12 CANPN6/10	295
Total elec. consumption	433
$CP_{E,CASE}$	23.3
η_{SWH}	9259%

Figure 14: Reduction in greenhouse gasses emissions (annual net) for different scenarios



by the saving of primary energy as well as the reduction of the Greenhouse Gases (GHG). The reduction of GHG for different scenarios is shown in Figure 14.

6. CONCLUSION

This study established that ADC-2 is feasible from the technical viewpoint for Jordan's weather. The investigation of CASE technology (ADC-2) in this work shows that this technology is more viable environmentally than for VCC, owing to the lower GHG emissions associated with VCC. When reusing the heat rejection from the CASE technology, the environmental feasibility becomes more appealing. The credits of GHG and carbon have been identified as a significant stimulate for using CASE technology, especially for the low tariffs of electricity.

REFERENCES

- Al-Maaitah, A.A.S., Al-maaitah, A.A. (2013), U.S. Patent No. 8,479,529. Washington, DC: U.S. Patent and Trademark Office.
- ECO-MAX. (2011), ECO-MAX™ Adsorption Chillers. Accessed from: <http://www.eco-maxchillers.com/common/content.asp?PAGE=383>.
- Fu, H., He, Q., Song, J., Shi, X., Hao, Y., Du, D., Liu, W. (2021), Thermodynamic of a novel advanced adiabatic compressed air energy storage system with variable pressure ratio coupled organic rankine cycle. *Energy*, 227, 120411.
- Giwa, A., Akther, N., Al Housani, A., Haris, S., Hasan, S.W. (2016), Recent advances in humidification dehumidification (HDH) desalination processes: Improved designs and productivity. *Renewable and Sustainable Energy Reviews*, 57, 929-944.
- Grossman, G. (2002), Solar-powered systems for cooling, dehumidification and air-conditioning. *Solar Energy*, 72(1), 53-62.
- Kojok, F., Fardoun, F., Younes, R., Outbib, R. (2016), Hybrid cooling systems: A review and an optimized selection scheme. *Renewable and Sustainable Energy Reviews*, 65, 57-80.
- Ma, Y., Morozjuk, T., Liu, M., Yan, J., Liu, J. (2019), Optimal integration of recompression supercritical CO₂ Brayton cycle with main compression intercooling in solar power tower system based on exergoeconomic approach. *Applied Energy*, 242, 1134-1154.
- Ratlamwala, T.A., Abid, M. (2018), Performance analysis of solar-assisted multi-effect absorption cooling systems using nanofluids: A comparative analysis. *International Journal of Energy Research*, 42(9), 2901-2915.
- Srikhirin, P., Aphornratana, S., Chungpaibulpatana, S. (2001), A review of absorption refrigeration technologies. *Renewable and Sustainable Energy Reviews*, 5(4), 343-372.
- World Bank. (2014), Development Indicators (WDI) Database. Accessed from: <http://www.devdata.worldbank.org/query/default.htm>.
- Youssef, P.G., Dakkama, H., Mahmoud, S.M., AL-Dadah, R.K. (2017), Experimental investigation of adsorption water desalination/cooling system using CPO-27Ni MOF. *Desalination*, 404, 192-199.
- Zhang, Y., Xu, Y., Zhou, X., Guo, H., Zhang, X., Chen, H. (2019), Compressed air energy storage system with variable configuration for accommodating large-amplitude wind power fluctuation. *Applied Energy*, 239, 957-968.